Spatially Variable (Microscopic) Model of the Drift Mobility for HgCdTe Diodes–Application in *TOSCA*

A. Schenk
Humboldt-Universität zu Berlin, Fachbereich Physik,
Institut für Optik und Spektroskopie,
Invalidenstraße 110, O–1040 Berlin, Germany

1 Introduction

In the small gap system $Hg_{1-x}Cd_xTe$ with $x \approx 0.2$ the drift mobility becomes a function of the local carrier density not only due to the doping profile but also as a consequence of degeneracy and screening. The latter features are important in highly doped regions of infrared photodiodes–all the Coulombic scattering mechanisms are effectively screened and, furthermore, all scattering processes depend directly on the position of the Fermi level. The commonly used factorization of the conductivity in the form 'charge density multiplied by a constant mobility' fails in this case. To overcome this drawback a fully microscopic mobility model has been established on the basis of Kohlers variational method (first momentum of the Boltzmann equation) which takes into account all relevant scattering mechanisms in $Hg_{0.8}Cd_{0.2}Te$. The Kohler variational method is right both for treating the inelastic optical-phonon scattering and for ending up with a numerical expense still suitable for application in device simulation programs. It was another goal to implement the model into the 2D simulator *TOSCA* to test its suitability and to study the physical effects in a selfconsistent calculation.

2 Analytical Model

The considered scattering mechanisms include polar optical (po), piezoelectric (pz), and acoustic (ac) phonon modes, ionized impurity scattering (cc), neutral impurity scattering (nc), alloy scattering (dis), and strain field scattering (sf). For clarity we restrict ourselves to the four dominant processes in the composition and temperature range of interest: po-, cc-, nc-, and sf-scattering. All expressions below hold for electrons, those for heavy and light holes follow immediately from $m_c \to m_{hh,lh}$, $n \to p_{hh,lh}$, and $\xi = kT/E_g \to 0$ in the case of heavy holes.

Alternatively to the invalid relaxation time approximation because of the inelastic po-scattering, the Kohler variational method [1] was applied. In first order, the mobility is determined by the 'golden rule' transition probabilities then. The scattering matrix elements were taken in the form with the Bloch factors set to 1. A Kane model was used for the band structure, and screening was described in Thomas-Fermi approximation including degeneracy [1]. For the po-scattering both HgTe-and CdTe-like longitudinal and transverse optical phonon modes were taken into account [2, 3]. The details of the scattering processes can be found in [2, 4] and the references therein.

The electron mobility is given by the expression

$$\mu_n = -\frac{16en}{9\pi\hbar^2} d_0^{-1}, \tag{1}$$

where n denotes the electron density and e the elementary charge. The quantity d_0, which contains all the information about the scattering processes, can be written in the following form:

$$\begin{aligned} d_0 &= \frac{m_c^2}{6(2\pi)^4\hbar^4}\int_0^\infty dE(\frac{d\gamma}{dE})^2\frac{\partial f}{\partial E}\{A^{nc}\frac{1}{2}\lambda^4\gamma^{*2}(E)+ \\ &+ A^{sf}\lambda^2[\gamma^*(E)+\frac{\gamma^*(E)}{1+\gamma^*(E)}-2\ln(1+\gamma^*(E))]+ \\ &+ A^{cc}[\ln(1+\gamma^*(E))-\frac{\gamma^*(E)}{1+\gamma^*(E)}]+ \\ &+ \sum_{i=1}^{2}\frac{A_i^{po}}{\omega_{LOi}}f_B(\omega_{LOi})\frac{1-f(E+\hbar\omega_{LOi})}{1+f(E)}\frac{[1+2\frac{E+\hbar\omega_{LOi}}{E_g}]}{[1+2\frac{E}{E_g}]}\times \\ &\times[\lambda^2\gamma^{*\frac{1}{2}}(E)\gamma^{*\frac{1}{2}}(E+\hbar\omega_{LOi})+g_+^i(E,\lambda)]\}. \end{aligned} \tag{2}$$

In (2) the following abbreviations were used:

$$\gamma(E)=E(\frac{E}{E_g}+1), \qquad \gamma^*(E)=\frac{4}{E_\lambda}\gamma(E), \qquad E_\lambda=\frac{\hbar^2\lambda^2}{2m_c}, \tag{3}$$

$$\lambda^2=\frac{e^2}{\epsilon_0\epsilon_s}[\frac{d}{d\eta_c}n+\frac{d}{d\eta_v}p], \quad \eta_c=F_n-(E_c-e\varphi), \quad \eta_v=E_v-e\varphi-F_p, \tag{4}$$

$$g_+^i(E,\lambda)=2\lambda^2\ln[\frac{q_{min}^2(E)+\lambda^2}{q_{max}^2(E)+\lambda^2}]+\lambda^4\frac{q_{max}^2(E)-q_{min}^2(E)}{(q_{max}^2+\lambda^2)(q_{min}^2+\lambda^2)}, \tag{5}$$

$$q_{\substack{min\\max}}^2(E)=\frac{2m_c}{\hbar^2}[\gamma^{\frac{1}{2}}(E+\hbar\omega_{LOi})\mp\gamma^{\frac{1}{2}}(E)]^2. \tag{6}$$

The meaning of the parameters in (2)–(6) is as follows: f–Fermi function, λ^{-1}–screening length, f_B–Bose function, $\hbar\omega_{LOi}$–LO-phonon energy of the i-th constituent, E_g–gap energy, ϵ_s–static dielectric function, $\eta_{c,v}$–electrochemical energies, $F_{n,p}$–quasi Fermi levels, $\varphi(\vec{r})$–electrostatic potential, and $E_{c,v}$–band edge energies. The quantities A^{nc}, A^{sf}, A^{cc}, and A^{po} result from the calculation of the transition matrix elements. They contain a variity of microscopic physical parameters, which all are available from experiment (for details see [4] and the references therein). The electrically active doping profile is included in A^{cc}.

The remaining integral in (2) could be solved analytically in the limits of nondegeneracy and total degeneracy under certain assumptions, but it was impossible to find a satisfactory interpolation for the transition region. Therefore, the last integration is carried out by a combination of the Gauss and the Laguerre method with only a few points.

In order to calculate the carrier densities very quickly, an interpolation formulae of Stahl [5] for the modified Fermi integral $J_{1/2}$

$$J_{1/2}(\eta,\xi)=\frac{2}{\sqrt{\pi}}\int_0^\infty dx\frac{[x(1+\xi x)]^{\frac{1}{2}}(1+2\xi x)}{1+\exp(x-\eta)} \tag{7}$$

($\xi = kT/E_g$) has been used, which differs from the exact result by less than 1% in the region ξ = [0 to 0.1]. The first derivative of this interpolation formula was used to determine the screening length after (4).

The model was carefully checked by comparing the theoretical results with experimental data of the electron and hole Hall mobilities [6, 3] over the whole temperature range. Since no difference between the Hall and drift mobility is obtained within the used order of the Kohler method, Hall factors both for impurity scattering and for the high temperature po-scattering were calculated to improve the check at least in the low and high temperature ranges. Due

to the uncertainty in some microscopic parameters resulting from published data by different authors, a final fit was possible within a factor of about 2. This should be much more than the error by the method itself. The fit served to fix the ambiguous microscopic parameters and led to a satisfactory agreement between the described model and measured mobilities in $Hg_{0.8}Cd_{0.2}Te$.

3 Numerical Results

The mobility model was implemented into the 2D device simulator *TOSCA* [7], which solves the van Roosbroeck system of semiconductor device equations by the method of finite elements [8, 9]. One is faced with a self-consistent problem, because the variables of these equations, the electrostatic potential $\varphi(\vec{r})$ and the carrier densities $n(\vec{r})$, $p(\vec{r})$ (or the quasi Fermi levels $F_n(\vec{r})$, $F_p(\vec{r})$, respectively), enter the mobility. A particular switch forces *TOSCA* to pass on the carrier densities and quasi Fermi levels, determined at each grid point by the main program, to the mobility subroutine. The electron and heavy hole mobilities (the contribution of light holes can be neglected) then are calculated for all grid points and enter the current matrix equations.

In order to demonstrate the major effects, a narrow, quasi 1D stripe with 213 vertices was chosen for the 2D domain, which had a size of $0.3 \times 11\mu m^2$. The doping profile was assumed to vary in y-direction only.

The concentration of assumed completely ionized residual impurities and the corresponding free carrier densities in a n^+n^-p junction of an infrared diode are shown in Fig. 1. For clarity, the set of microscopic parameters was chosen such, that po- and cc-scattering dominate (nc- and sf-scattering suppressed).

The resulting mobility profiles for electrons and heavy holes in thermodynamic equilibrium are given in Fig. 2. These profiles can be interpreted in the following way: Within the n^+-region the electron gas is highly degenerate, and screening results in a large electron mobility value, despite the scatterer concentration is high. The profile is constant there, because the degeneracy is total. In the n^+n^--region screening becomes less efficient, and the electron mobility goes down reaching its minimum in the depletion layer. In the p-region both kinds of carriers are nondegenerate. The electron mobility follows the decrease in the total impurity concentration there, reaching a maximum at the p-contact. A detailed analysis shows, that cc-scattering dominates the electron mobility over the whole structure.

In the case of heavy holes the cc-scattering dominates only in the n^+-region. The hole mobility directly reflects the impurity profile there. Within the n^-p-region the po-scattering is the most important one. Since screening has only little effect here, the hole mobility becomes almost constant. It follows from Fig. 2, that both mobility profiles vary over one order of magnitude.

Fig. 3 demonstrates the change in the electron mobility profile, if an external voltage is applied. A forward bias injects electrons into the n^--region, where they become more and more degenerate. The mobility increases with rising voltage. At $U = 0.1V$ its value in the n^--region becomes larger than the unchanged one in the n^+-region because of the lower impurity concentration in this part of the junction. A new maximum emerges distingtly in the p-region, where degeneracy effects come into play at higher biases, but at the same time the Fermi level remains pinned on the p-side boundary, since the p-contact was taken as ideal Ohmic.

Obviously, the averaged electron mobility (as average over the whole device) increases with rising positive voltage. The mobility itself becomes a function of the external voltage.

If the diode is reverse biased, the mobility profile changes only within the depletion region. It decreases slightly due to the rising depletion, and the "mobility well" broadens to the same extent as the depletion region.

The forward I-U characteristic of the investigated diode is shown in Fig. 4. For comparison,

results with three constant values of the electron mobility are also presented. No constant averaged mobility value can reproduce the correct I-U characteristic over the whole positive voltage axis. At biases higher than 50 mV a strong deviation from the presented model occurs. This is due to the injection of majority carriers accompanied by an increase of the averaged mobility.

4 Summary

The local mobility in a $Hg_{0.8}Cd_{0.2}Te$ photodiode is determined by the doping profile, by the dominating scattering mechanisms, and by degeneracy and screening effects. All these effects were described in a microscopic model, which was incorporated into the 2D device simulator *TOSCA*. Since the mobility depends on the carrier density, except Boltzmann statistics holds utterly, its profile may change with applied voltage. This leads to an increasing averaged mobility in the case of majority carrier injection. I-U curves become steeper than they would be using a constant mobility value.

Acknowledgement

The author is indebted to Prof. H. Gajewski from Karl-Weierstrass-Institute of Mathematics, Berlin, who implemented the mobility routine into the 2D device simulator *TOSCA*. The unceasing cooperation with him and his collaborators is gratefully acknowledged.

References

[1] W. Brauer and H.-W. Streitwolf, Theoretische Grundlagen der Halbleiterphysik, Akademie-Verlag, Berlin 1977 (p.166).

[2] J. J. Dubowski, T. Dietl, W. Szymanska, and R. R. Gałazka, J. Phys. Chem. Solids **42**, 351 (1981), and references therein.

[3] P. Höschl, P.Moravec, V. Prosser, V. Szöcs, and R. Grill, phys. stat. sol. (b) **145**, 637 (1988).

[4] A. Schenk, phys. stat. sol. (a) **122**, 413 (1990), and **122**, 723 (1990).

[5] M. Stahl, unpublished.

[6] W. Hoerstel and A. Schmiede, private communication.

[7] H. Gajewski, *TOSCA*-Handbook, Berlin 1989.

[8] W. van Roosbroeck, Bell. Syst. tech. J. **29**, 560 (1950).

[9] P. A. Markowich, The Stationary Semiconductor Device Equations, Springer-Verlag, 1985 (p.133).

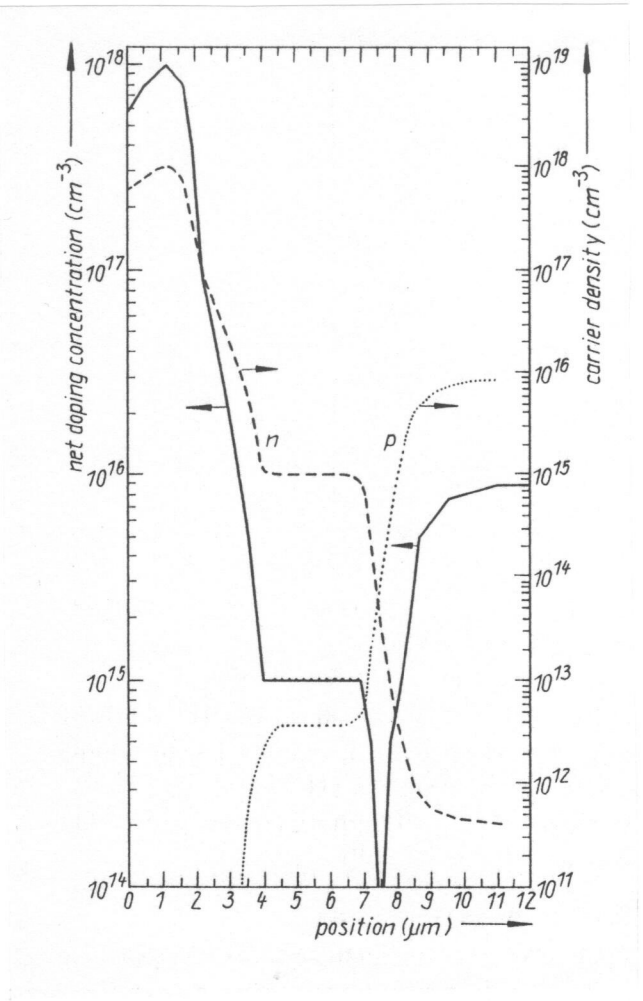

Figure 1: Net doping profile of the assumed, completely ionized, residual impurities of the n^+n^-p junction (—) and the corresponding free carrier densities

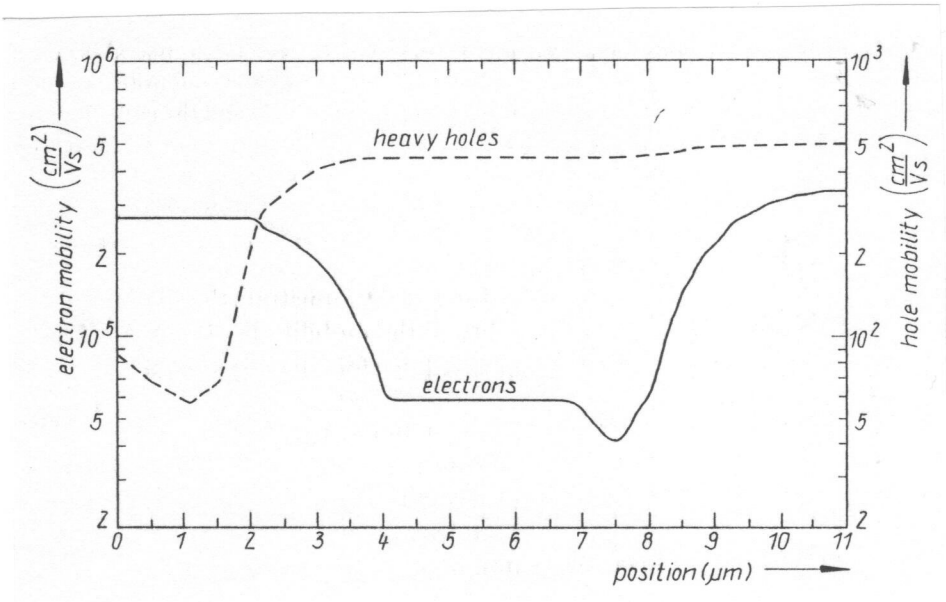

Figure 2: Electron and heavy hole mobility profiles of the junction of Fig. 1. Only po- and cc-scattering were taken into account

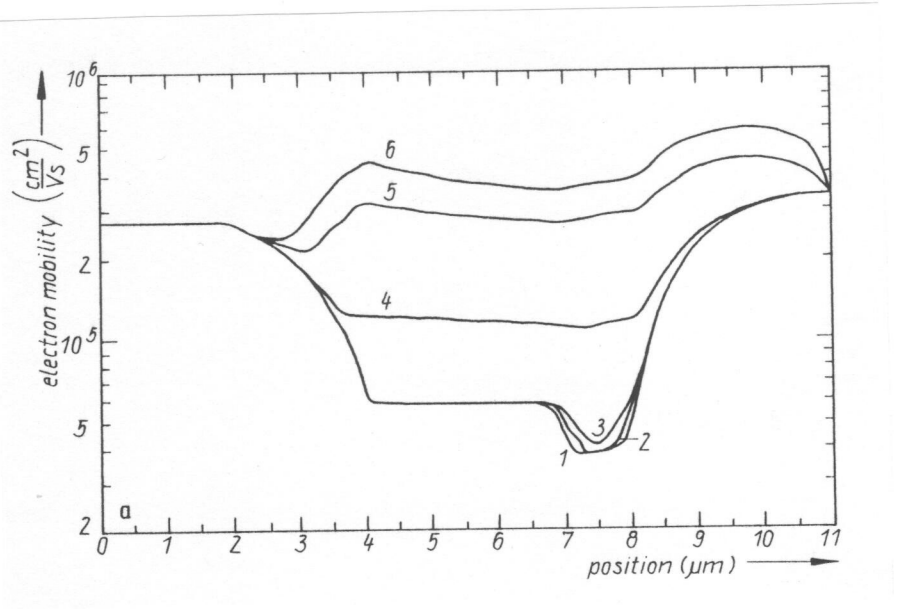

Figure 3: Electron mobility of the n^+n^-p junction for different applied voltages: (1) -200 mV, (2) -100 mV, (3) 0 V, (4) +50 mV, (5) +100 mV, (6) +150 mV

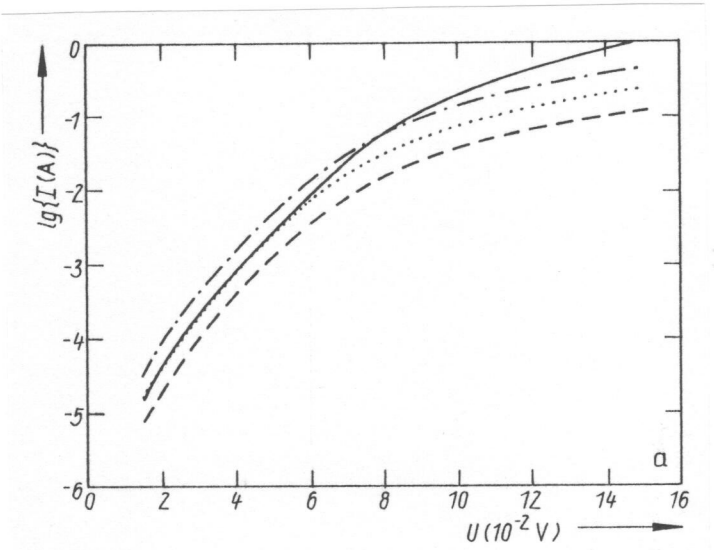

Figure 4: Comparison of the I-U characteristics of the n^+n^-p junction with spatially variable model (—) and with constant electron mobilities: $1 \times 10^5 cm^2/Vs$ (- - -), $2 \times 10^5 cm^2/Vs$ ($\cdots$), $4 \times 10^5 cm^2/Vs$ ($- \cdot -$). The constant heavy hole mobility is $\mu_{hh} = 300 cm^2/Vs$